Journal of Ceramic Processing Research. Vol. 24, No. 5, pp. 807~815 (2023)
(Received 27 June 2023, Received in revised form 15 August 2023, Accepted 29 August 2023)
https://doi.org/10.36410/jcpr.2023.24.5.807

J O U R N A L O F
Ceramic Processing Research

Effect of Rutile/Anatase TiO_2 on surface properties of ZnO-Al_2O_3-CaO-SiO_2 glass system

Dongchan Kim, Seunggu Kang and Kangduk Kim*
Department of Advanced Material Engineering, Kyonggi University, Suwon, Korea

In this study, we investigated the effects of dimorphous nucleating agents–rutile TiO_2 and anatase TiO_2, on the crystallization and surface properties of ZnO-Al_2O_3-CaO-SiO_2-based glass. Glass specimens were prepared by substituting rutile TiO_2 and anatase TiO_2 at 1, 3, and 5 wt.% and subsequently heat treating at 1050 °C for 90 min to induce crystallization. The crystallization characteristics and surface properties of the crystallized glass were analyzed using X-ray diffraction (XRD), scanning electron microscopy (SEM), gloss, Fourier-transform infrared (FTIR) spectroscopy, hardness, and colorimetric analyses. The XRD and SEM analyses revealed the presence of a titanite crystalline phase in the glass matrix. However, the addition of anatase TiO_2 as a nucleating agent resulted in a significant decrease in glossiness. FTIR deconvolution in the range of 800-1300 cm^{-1} showed an increase in the degree of [SiO_4] tetrahedral polymerization with higher levels of crystallization. micro-Vickers hardness of the glass specimens increased from the original value of 6.32 GPa to a maximum of 7.05 GPa, indicating enhanced hardness due to crystallization. Colorimetric analysis indicated that the inclusion of rutile TiO_2 as a nucleating agent increased the Yellow Index of anatase TiO_2.

Keywords: Glass-ceramics, Crystallization, Rutile/Anatase TiO_2, Surface properties.

Introduction

TiO_2 is a transition metal oxide widely used in various industries. Among its different polymorphs, rutile TiO_2 is the most thermodynamically stable, whereas anatase and Brookite TiO_2 are considered metastable forms. Rutile and anatase TiO_2 are the most used opacifiers, particularly in the pigment and ceramic industries [1-3]. In ceramics containing CaO and SiO_2, TiO_2 readily reacts to form the titanite ($CaTiSiO_5$) phase. However, unreacted TiO_2 fails to entirely participate in the reaction and undergoes transformation into the rutile phase, which contributes to the yellowing phenomenon [4-5]. Moreover, controlling the generated rutile phase, which is sensitive to impurities, sintering atmosphere, and various other conditions, was initially challenging, limiting its practical applications [6]. However, with advancements in industrial processes facilitating better control over material purity and process parameters, the yellowing phenomenon has been suppressed. This has led to the increased utilization of TiO_2 as an opacifier and has attracted significant research attention, particularly in its role as a nucleating agent in glass manufacturing [7].

Yu et al. [8] reported that the addition of TiO_2 as a nucleating agent in CaO-MgO-P_2O_5-SiO_2 -based glass reduced the crystallization temperature and significantly decreased the activation energy required for crystallization by more than 100 kJ/mol compared to the conventional parent glass. This effective reduction in the activation energy facilitated the promotion of crystallization. Mukherjee et al. [9] observed the formation of three-dimensional and uniform crystalline phases in SiO_2-$3Al_2O_3$-$3CaO$-based glass with the addition of 6-12 wt.% TiO_2. Further, they reported an increase in density (2.56-2.93 g/cm^3) and surface hardness (5.87-6.63 GPa) due to crystallization. Nucleating agents, such as TiO_2 reduce the viscosity of glass at high temperatures and promote nucleation and crystal growth. In addition, in silicate-based glasses, they induce bulk crystallization and decrease the maximum crystallization temperature. Therefore, the inclusion of Ca, Si, and Ti ions in the composition facilitates the formation of the titanite crystalline phase owing to thermal treatment [9-12].

In this study, we investigated the surface properties and color manifestation differences resulting from the crystallization behavior induced by the nucleating role of dimorphous TiO_2 (rutile, and anatase) substitution in the ZnO-Al_2O_3-CaO-SiO_2-based glass, which is extensively used in the ceramic industry as a universal frit. Furthermore, we investigated the structural influence of each TiO_2 specimen for a given composition by analyzing the FTIR spectra.

*Corresponding author:
Tel : +82-10-6206-6290
E-mail: solidwaste@kyonggi.ac.kr

Experimental Procedure

An industrial frit (parent glass; PG) based on the ZnO-Al_2O_3-CaO-SiO_2 system, commonly used by company 'H' in Korea, was employed. The chemical compositions of the glasses are listed in Table 1. Rutile TiO_2 (Kojundo Chemicals, Ltd., Japan: 3N, ca 2 μm) and anatase TiO_2 (Kojundo Chemicals, Ltd., Japan: 2N) were substituted as nucleating agents for glass crystallization, and the mixing ratios are listed in Table 2. After weighing the raw materials according to the mixing ratios, dry milling was performed for 12 h with zirconia balls (Φ=5, 10 mm). The mixed powders were then heated at a rate of 3 °C/min and maintained at 1050 °C for 90 min to produce crystallized specimens.

To analyze the crystal phases of the specimens, X-ray diffraction (XRD) measurements were performed using a D8 ADVANCE instrument (Bruker Co., USA), and the crystallinity was analyzed using DIFFRAC.EVA software (Bruker Co., USA). Thermal analyses of the specimens were conducted using a simultaneous thermal analysis-mass spectrometry (STA-MS; STA 409PC-QMS 403C, Netzsch, Germany) via differential thermal analysis (DTA). The microstructures of the polished specimens were observed using field-emission scanning electron microscopy (FE-SEM; Nova NanoSEM450, FEI company, USA) after etching the specimens in a 3% HF solution for 10 s. Energy-dispersive X-ray spectroscopy (EDS; Noran System 7, Thermo Scientific, USA) was performed to analyze the crystal phases observed in the SEM images. The surface hardness of the specimens was measured five times under a 0.2 kgf/10s load using a micro-Vickers hardness tester (VH1102, Wilson, USA) as per the ASTM-E384-17 standard. The surface gloss of the specimens was measured using a gloss meter (Novo-Gloss Trio, Rhopoint Instrument, UK), and glossiness was measured at reflection angles of 20°, 60°, and 85°, according to the ISO-2813:2014 standard. The color variations of the specimens were measured using a precision colorimeter (NR100, 3nh, Shenzhen, China). Crystallized specimens were ground to size less than 45 μm and then prepared as KBr pellets for FTIR analysis in the range of 400-2000 cm^{-1} using an FTIR spectrometer (IRTracer-100, Shimadzu, Japan).

Table 1. The Chemical composition of parent glass.

Component	wt(%)
SiO_2	59.38
ZnO	9.93
Al_2O_3	9.53
CaO	7.31
K_2O	3.90
BaO	2.49
Na_2O	2.02
ZrO_2	1.01
MgO	0.89
Fe_2O_3	0.16
L.O.I	3.37
Total	100

Table 2. The batch composition of specimens.

Specimen	Composition (wt%)		
	Original glass	Rutile TiO_2	Anatase TiO_2
PG	100	-	-
T1	99	1	-
T3	97	3	-
T5	95	5	-
AT1	99	-	1
AT3	97	-	3
AT5	95	-	5

Results and Discussion

Fig. 1 shows the DTA results of PG and the XRD results of PG heat-treated at 1050 °C. PG appeared amorphous after heat treatment, and during TG/DTA analysis, a heat release peak attributed to the combustion of organic matter and a weight loss of approximately 2.24% are observed at approximately 400 °C.

Fig. 2 shows the XRD patterns of the samples with various compositions (Table 2) heat-treated at 1050 °C for 90 min. Regardless of the type of TiO_2 nucleating agent, the presence of a titanite crystalline phase ($CaTiSiO_5$, ICSD:98-008-9744) was evident when the substitution amount exceeded 3 wt.%. Furthermore, an increase in peak intensity was observed as the substitution amount increased.

Fig. 3 shows the variation in crystallinity with respect to the change in TiO_2 content based on the XRD patterns shown in Fig. 2. The analysis was performed using the DIFFRAC.EVA program, based

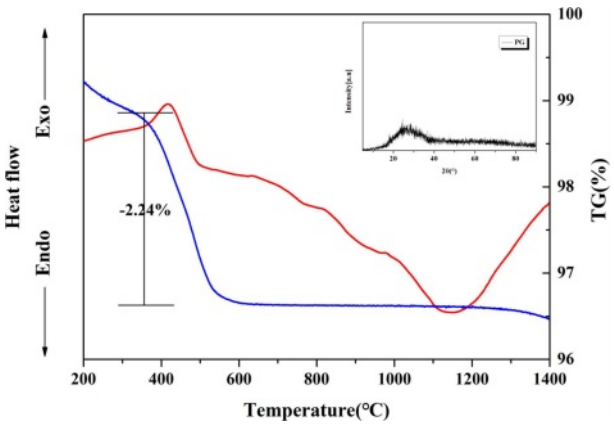

Fig. 1. DTA curve and XRD pattern of PG.

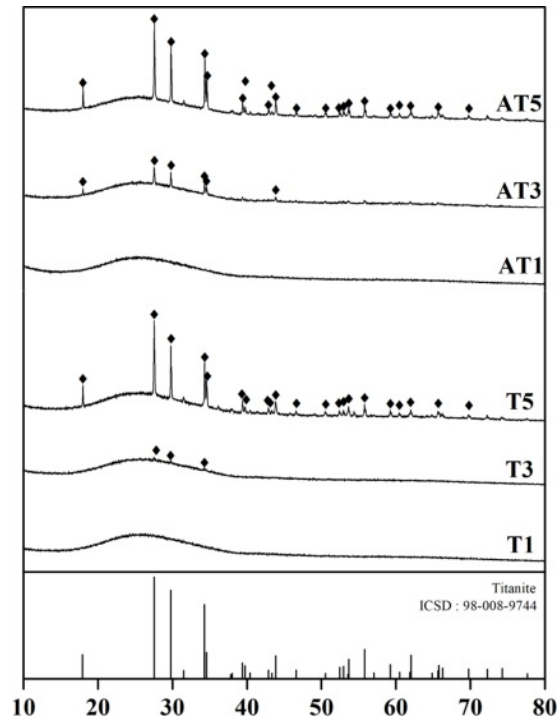

Fig. 2. XRD patterns of specimens heat-treated at 1050 °C.

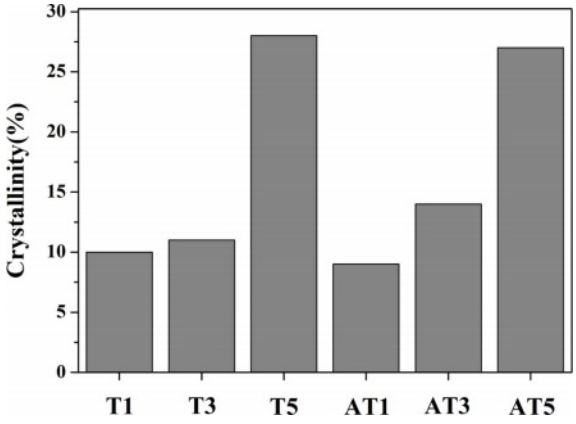

Fig. 3. Crystalline and amorphous fraction of specimens heat-treated at 1050 °C.

on the Benedetti equation [13]:

$$\text{Crystallinity}(\%) = \frac{A_c}{A_c + A_a} \times 100 \quad (1)$$

where A_c is the crystalline region observed in the XRD pattern and A_a is the amorphous region. With the substitution of rutile TiO_2, the degree of crystallinity increases from 10% to 28%, whereas, with the substitution of anatase TiO_2, it increases from 9% to 27%. The nucleating agent had no significant effect on the crystallinity. In a study by Sheikhattar et al. [14], a commercial glass containing 17 wt.% TiO_2 exhibited a crystallinity of 12.8% when heated at 1040 °C for 40 min. Danewalia et al. [15] reported that SiO_2-CaO-Na_2O-P_2O_5-Fe_2O_3-MnO_2 glass composition with TiO_2 added in the range of 1.25-10 wt.% exhibited a crystallinity of 19-25% when heat-treated at 850-900 °C for 2 h. According to Zitani et al. [16], the CaO-MgO-TiO_2-SiO_2 glass composition exhibited a crystallinity of above 80% when heat-treated at 850-950 °C for 4 h. Various glass compositions with TiO_2 as a nucleating agent showed crystallinities in ranges of 11.3%-25.4% in cases of low crystallinity and 85%-92% in cases of high crystallinity, depending on the heat-treatment conditions. Therefore, considering the relatively short heat treatment time observed in this study after the addition of the nucleating agent, we concluded that the observed crystallinity was relatively low.

Fig. 4 shows the surface microstructure of the specimens heat-treated at 1050 °C for 90 min, observed via SEM. In contrast to the smooth surface of PG, increasing the substitution amount of each nucleating agent increases the number and distribution of wedge-shaped crystals. The size of the crystals increased to approximately 5 μm with the addition of nucleating agents. When the crystallinity increased, the distribution and number of crystals increased; consequently, the generated crystals grew in random directions and merge with adjacent crystals. This phenomenon created irregularly shaped crystals that were different from their original form; this became one of the factors contributing to the enhancement of the mechanical strength of the glass [17, 18].

Fig. 5 shows the results of the EDS analysis of the T5 and AT5 specimens, which exhibited a significant number of crystals (Fig. 4). The EDS analysis was conducted separately for the crystals and glassy phase. The crystals exhibited the same composition as titanite ($CaTiSiO_5$), as confirmed by the XRD analysis, whereas the glassy phase had the same chemical composition as that of PG.

Fig. 6 shows the results of the surface glossiness analysis of the specimens heat-treated at 1050 °C for 90 min. As the crystallization of the glass progressed, glossiness decreased from the initial value of 82.26 GU to a maximum of 51.16 GU. Furthermore, a rapid decrease in glossiness was observed in the specimens with anatase TiO_2 substitution compared with those with rutile TiO_2 substitution. Wang et al. [19] reported an increase in surface hardness but a decrease in glossiness with the manifestation of anorthite crystals in the glass composition as the crystallinity increased. Banijamali et al. [20] reported surface whitening as crystallization progressed in a CaO-Al_2O_3-SiO_2 (CAS) glass composition with various amounts of CaF_2 and B_2O_3 additives. In this study, the decrease in glossiness of the specimens was due to the crystallization of the glass caused by heat treatment. In addition, we presumed that the abrupt decrease in glossiness observed in the specimens with rutile TiO_2 substitution compared with those with anatase TiO_2 was due to the higher reflective index of rutile TiO_2 (Refractive indices of rutile TiO_2

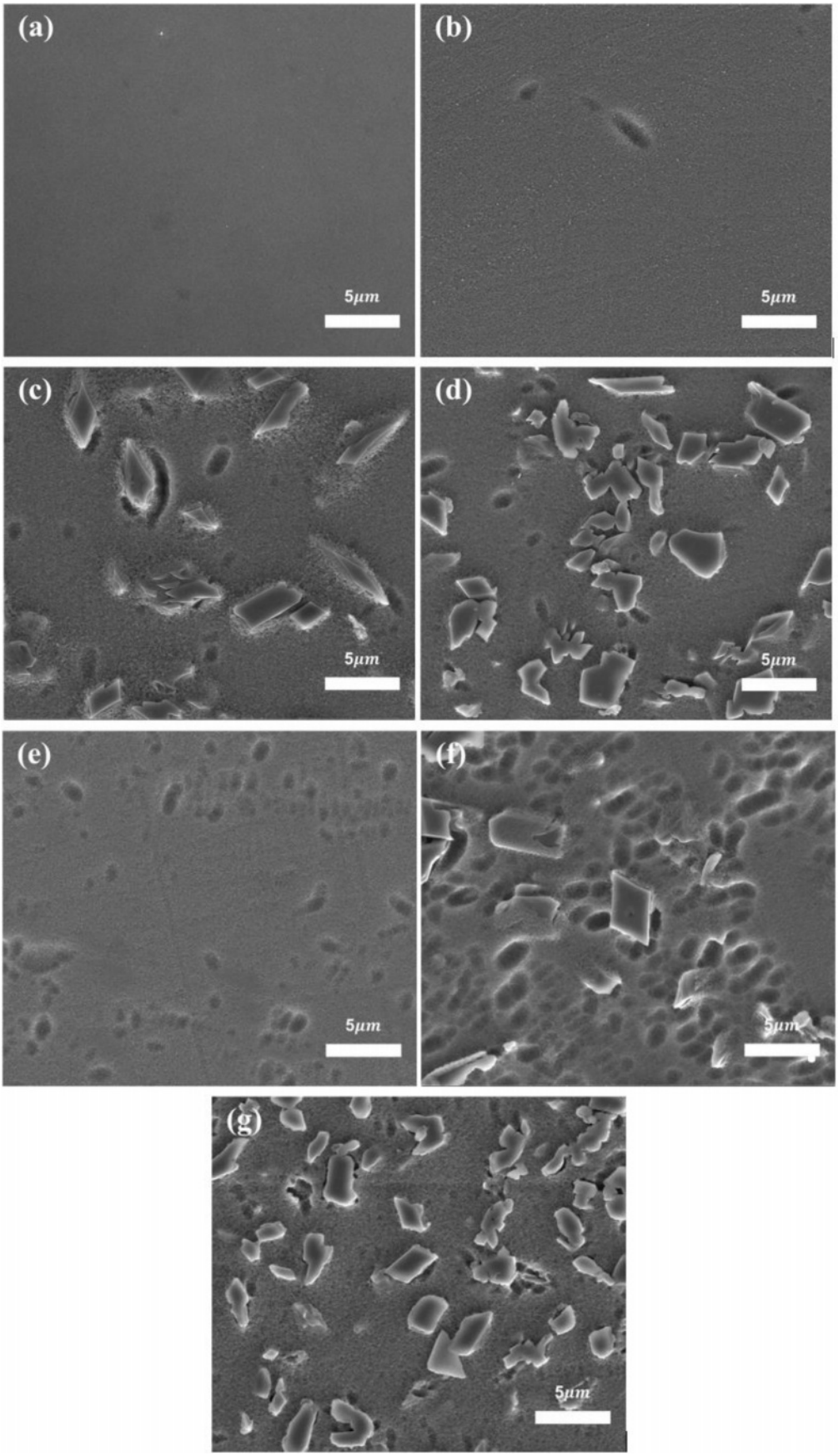

Fig. 4. SEM micrographs of surface of specimens heat-treated at 1050 °C; (a) PG, (b) T1, (c) T3, (d) T5, (e) AT1, (f) AT3 and (g) AT5. The specimen was etched with 3 wt% hydrofluoric acid solution for 10 s.

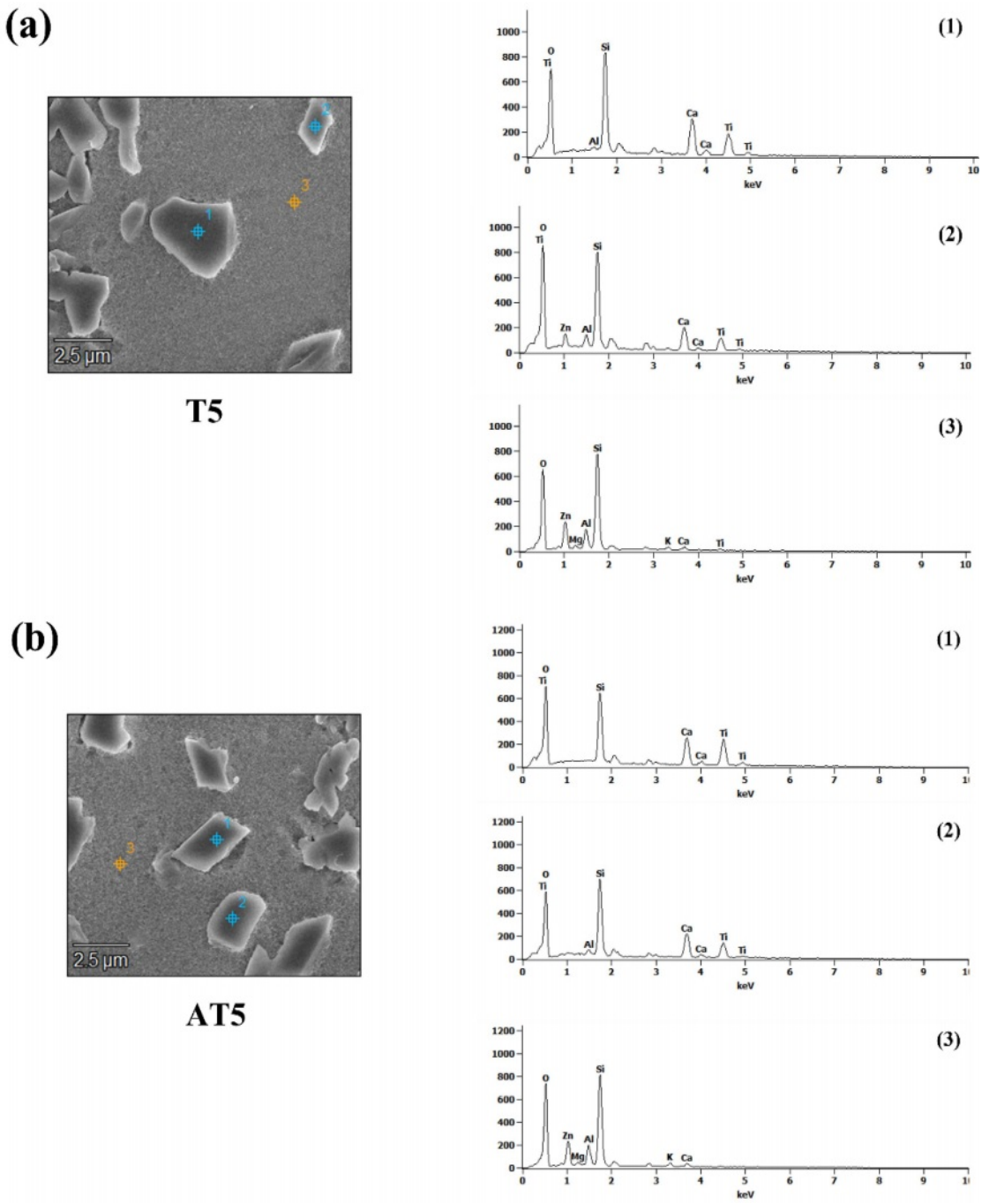

Fig. 5. SEM micrographs and EDS analysis of (a) T5, (b) AT5 specimen heat-treated at 1050 °C.

and anatase TiO_2 are 2.75 and 2.55, respectively) [21, 22].

Table 3 and Fig. 7 show the results of the whiteness and yellowness analyses conducted on the surfaces of the heat-treated specimens. Initially, the L^* (light to dark axis), a^* (red to green axis), and b^* (yellow to blue axis) values were measured 10 times, and the yellow index (yellowness) was determined as per ASTM E313-96 D65/10. The L^* and b^* values, which are associated with the appearance of white and yellow on the ceramic surface, increased proportionally within the ranges of 91.52-93.41, and 2.65-4.51, respectively, as the substitution level increased regardless of the type of nucleating agent. In particular, L^*, which is associated with the appearance of white, was higher in the specimens with anatase TiO_2 substitution, whereas b^*, which is associated with that of yellow, was higher in the specimens with rutile TiO_2 substitution. Compared to the original PG value of 34.43, the yellowness of the specimens with anatase TiO_2 substitution increased to a maximum of 34.26, whereas the specimens with rutile TiO_2 substitution exhibited a higher value, reaching a

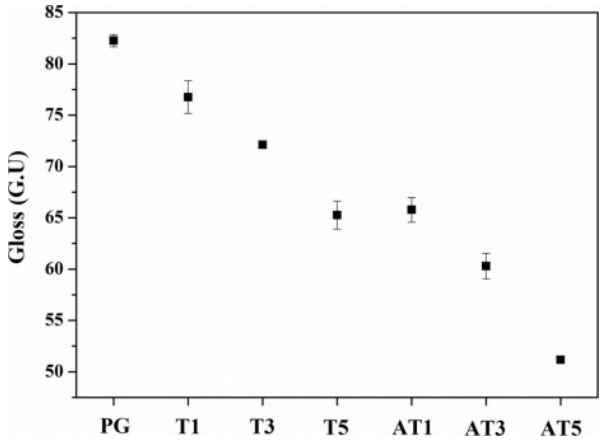

Fig. 6. Gloss Unit (GU) of specimens heat-treated at 1050 °C.

Table 3. Colour (L^*, a^*, b^*) values of specimens.

Specimen	L^*	a^*	b^*
PG	92.11	-1.13	3.17
T1	91.52	-1.22	2.65
T3	91.96	-1.12	3.09
T5	92.57	-1.05	4.51
AT1	92.12	-1.32	2.69
AT3	92.61	-1.06	3.05
AT5	93.41	-1.14	3.08

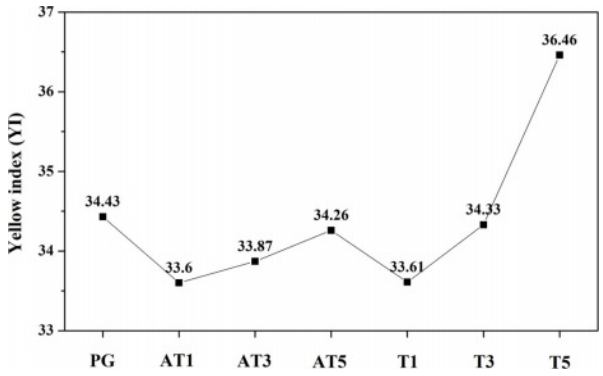

Fig. 7. Yellow index (YI) values of specimens heat-treated at 1050 °C.

maximum of 36.46, surpassing that of PG. Teixeira et al. [23] reported an increase in reflectance owing to the presence of titanite crystals formed when ZrO_2 was substituted with rutile/anatase TiO_2 in silicate-based frit compositions and observed that the use of anatase TiO_2 facilitated the production of white glazes compared to specimens using rutile TiO_2. Previous studies suggest an effect in promoting the whiteness of glass surfaces with respect to the titanite crystalline phase observed in this study [24, 25]. In particular, specimens substituted with anatase TiO_2 exhibited a higher gloss owing to variations in the refractive index, coupled with an increase in whiteness attributed to the presence of the

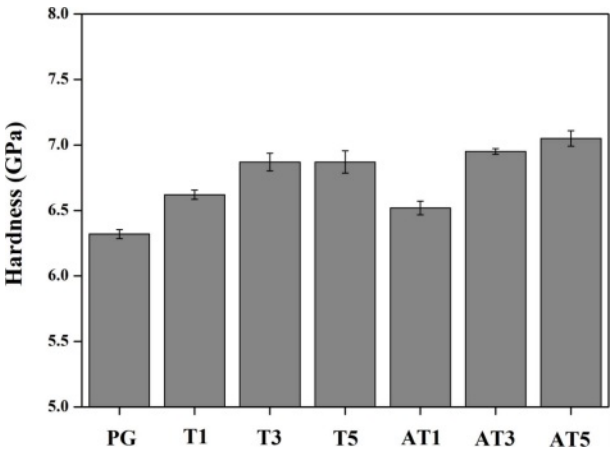

Fig. 8. Micro-Vickers hardness of specimens heat-treated at 1050 °C.

titanite crystalline phase. In contrast, rutile TiO_2, which causes yellowing, contributed to a higher level of yellowness in specimens substituted with this nucleating agent. Thus, substitution with rutile TiO_2 resulted in a higher level of yellowness compared to the specimens substituted with anatase TiO_2.

Fig. 8 shows the results of surface hardness analysis

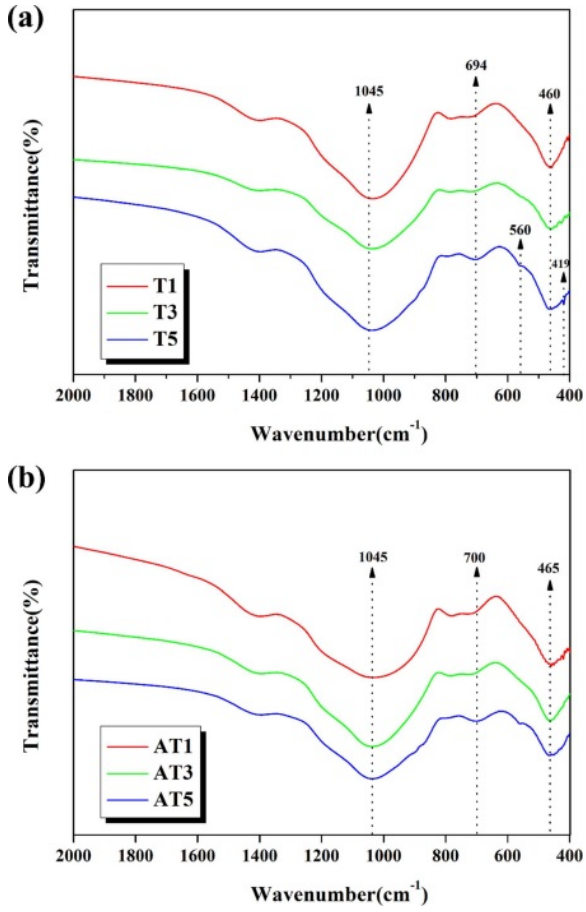

Fig. 9. FT-IR spectrum of specimens with heat-treated at 1050 °C; (a) T1, T3, T5, (b) AT1, AT3, AT5

for each heat-treated specimen. The surface hardness increased as the substitution amount of TiO_2 increased, reaching the highest values of 7.05 GPa for AT5 and 6.87 GPa for T5, compared with the surface hardness of the original PG (6.32 GPa). This increase could be associated with an increase in crystallinity owing to the crystallization of the glass. Banijamali et al. [20] reported that the hardness increased as the crystallinity of the glass increased by approximately 11% in a CaO-CaF_2-Al_2O_3-SiO_2 glass system. Further, Miyata et al. [26] reported increased size and crystallinity of Gahnite ($ZnAl_2O_4$) crystals and a maximum hardness value of 7.02 GPa in crystallized glass when the ZnO-Al_2O_3-SiO_2 glass composition was sintered at 950 °C for 1-6 h.

Fig. 9 shows the results of the FTIR analysis of the bond structure of the crystallized specimens induced by the nucleating agent. The broad spectra observed at approximately 460-465, 560, and 1045 cm^{-1} are associated with the SiO_4 tetrahedral structure bonding [27-28].

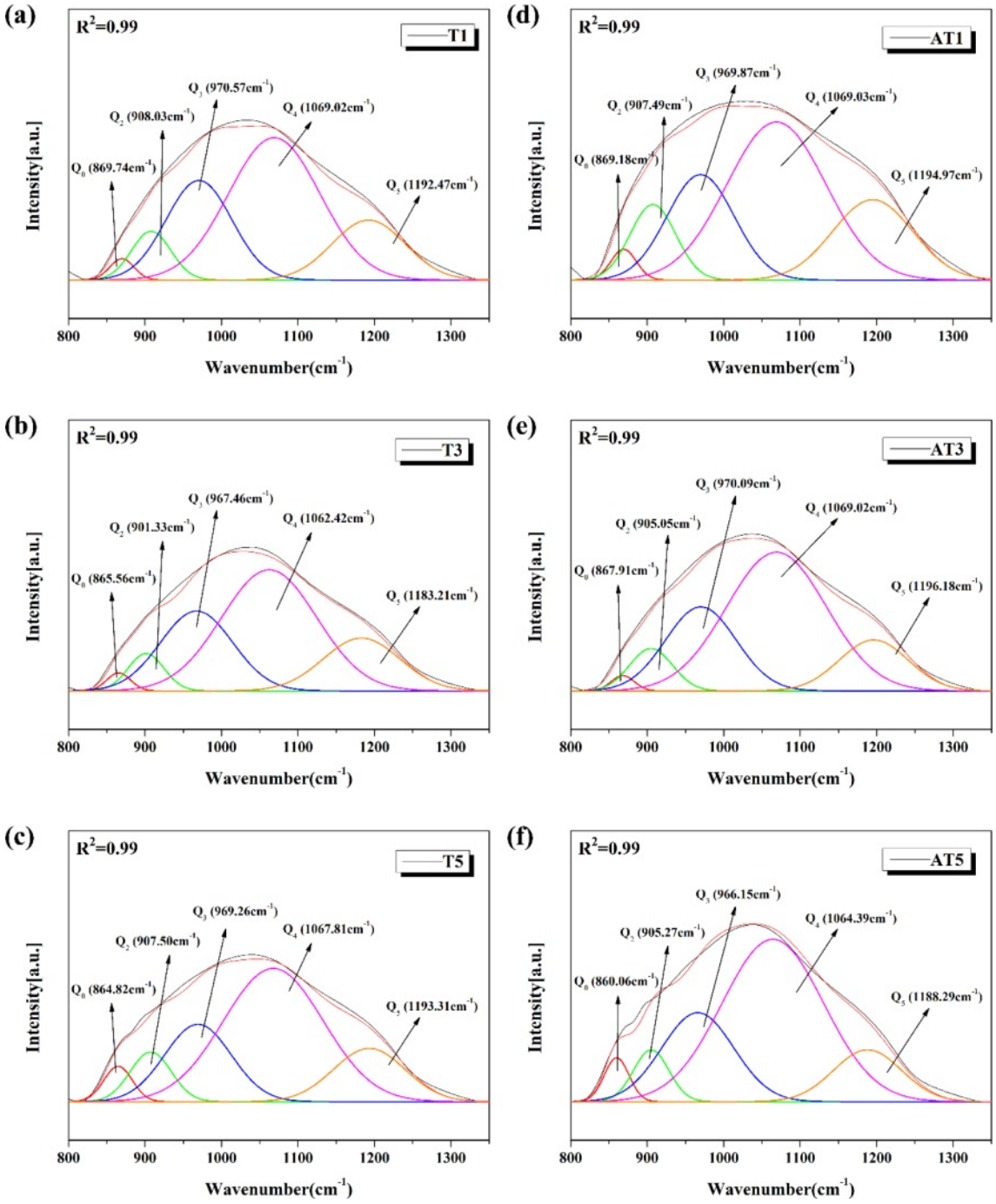

Fig. 10. Representative deconvolution results of FT-IR spectra in the range of 800-1300 cm^{-1}; (a) T1, (b) T3, (c) T5, (d) AT1, (e) AT3 and (f) AT5.

The absorption peak observed at 694-700 cm^{-1} is due to the TiO_6 octahedral structure bonding [29]. As the substitution level of each type of TiO_2 increased, the bonding strength of the TiO_6 octahedral structure, which constitutes the titanite ($CaTiSiO_5$) crystal phase, increased. Moreover, a sharper peak for Si-O bond is observed in the crystallized glaze with higher crystallinity, particularly in the anatase TiO_2-substituted glaze.

Fig. 10 shows the results of Gaussian deconvolution of the broad peak observed in the wavelength range of 800-1300 cm^{-1}, based on the FTIR spectra shown in Fig. 9. The degree of polymerization of the SiO_4 tetrahedral structural bonding in the glass was calculated using the peaks in this range, which demonstrated the changes in the glass network structure according to the crystallization tendency of the glass. The degree of polymerization of the glass network is generally estimated by the relative content of the Q_n-species (n = 0, 1, 2, 3, and 4), which represents the number of bridged oxygen atoms in a [SiO_4] unit. The relative ratios of the deconvoluted areas of each Q_n unit can be used to qualitatively compare the degree of polymerization of the glass composition [30-32]. According to Zhao et al. [33], as the Fe_2O_3 content in the CMAS glass composition increased, the crystallinity of the glass decreased, and the polymerization degree (Q_1+Q_2/Q_3 area ratio) increased. This shows that the structural change in the glass is closely related to the crystallinity and degree of polymerization. According to Xu et al. [34], the addition of CeO_2 to CMAS-based glass results in a significant correlation between the crystallization characteristics and structural changes in the glass. Previous studies revealed that a decrease in the degree of glass polymerization impeded the formation of the silica-oxygen network, consequently resulting in a reduction in the crystallinity of the diopside ($MgCaSi_2O_6$) crystalline phase. Generally, Q_1 and Q_2 units, which exist in monomeric and dimeric forms, respectively, contribute to the depolymerization of the glass structure,

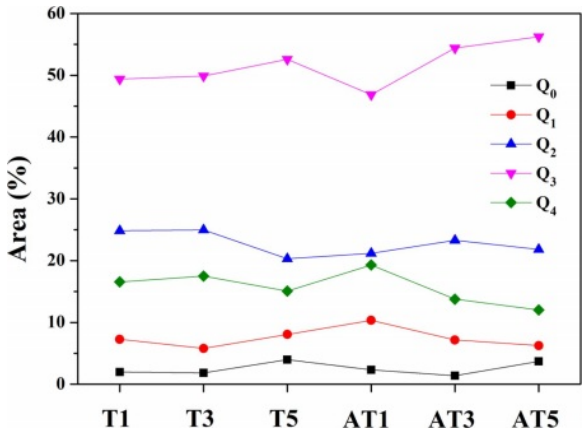

Fig. 11. The abundance of Q_n fraction of specimens heat-treated at 1050 °C.

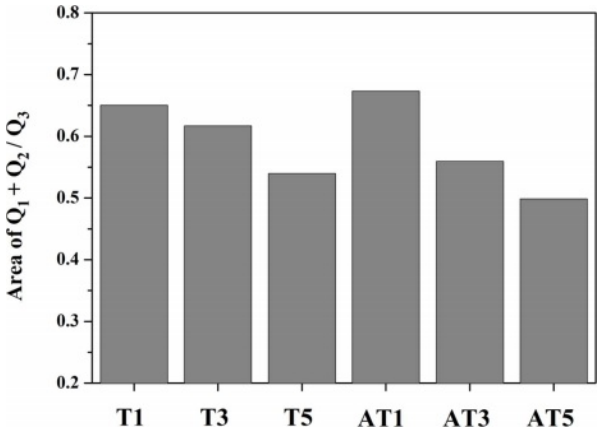

Fig. 12. Area ratio of Q_3/Q_1+Q_2 obtained from a Gaussian deconvolution of the FTIR spectra.

whereas Q_3 units, which exist in layered forms, contribute to increasing the degree of polymerization of the glass structure [33, 35].

Figs. 11 and 12 depict the areas of each Q_n unit and the Q_1+Q_2/Q_3 area ratio of the glass composition. Fig. 11 indicates that, regardless of the type of nucleating agent, the area of the Q_3 unit increases proportionally as the substitution level increases. In addition, Fig. 12 shows that as crystallization progressed, the degree of polymerization of the specimens increased, and the Q_1+Q_2/Q_3 area ratio decreased. In our study, we determined that TiO_2 substitution as a nucleating agent increases the degree of polymerization of the glass structure, and also enhances crystallization, leading to improvements in mechanical strength, including hardness.

Conclusion

1) ZnO-Al_2O_3-CaO-SiO_2 glass composition was thermally treated at 1050 °C after substitution with two types of nucleating agents: rutile and anatase TiO_2. The formation of a titanite crystalline phase occurred, and the degree of crystallization of the glass increased in the range of 9%-28% as the nucleating substitution agent content increased.

2) The degree of polymerization of the [SiO_4] tetrahedral structure in each specimen, as analyzed by FTIR, correlated with the increasing degree of crystallization. Moreover, the specimens with anatase TiO_2 substitution exhibited a higher degree of polymerization than those with rutile TiO_2 substitution. Further, a maximum hardness of 7.05 GPa was observed in the specimens with anatase TiO_2 substitution, which was slightly higher than those with rutile TiO_2 substitution.

3) Color analysis revealed that the anatase TiO_2 substituted-specimens had higher L^* values, whereas the anatase TiO_2 substituted-specimens had higher b^* values. The use of anatase TiO_2 as a nucleating agent effectively suppressed discoloration and improved the

whiteness of the glass composition compared to rutile TiO_2. However, in terms of glossiness, the specimens with anatase TiO_2 substitution exhibited lower values owing to differences in the refractive index.

Declaration of Competing Interest

The authors declare that they have no known competing financial interests or personal relationships that could have appeared to influence the work reported in this paper.

Acknowledgements

This work was supported by Kyonggi University's Graduate Research Assistantship 2023.

References

1. A.J. Haider, Z.N. Jameel, H.M. Imad, and Al-Hussaini, Energy Procedia 157 (2019) 17-29.
2. M.J. Gázquez, J.P. Bolívar, R. García-Tenorio, and F. Vaca, Sci. Res. 5 (2014) 441-458.
3. R.E. Day, Polym. Degrad. Stab. 29[1] (1990) 73-92.
4. G. Biffi, G. Ortelli, and P. Vincenzini, Ceram. Int. 1 (1975) 34-35.
5. S.K. Chen and H.S. Liu, J. Mater. Sci. 29 (1994) 2921-2930.
6. Pigments, Titanium Dioxide. "Manufacture and General Properties of Titanium Dioxide Pigments." (London: Tioxide Group 1999).
7. H.R. Fernandes, D.U. Tulyaganov, and J.M.F. Ferreira, J. Mater. Sci. 48[2] (2013) 765-773.
8. B. Yu, K. Liang, A. Hu, and S. Gu, Mater. Lett. 56[4] (2002) 539-542.
9. D.P. Mukherjee and S.K. Das, Ceram. Int. 40[3] (2014) 4127-4134.
10. Y.R. Rho, K.D. Kim, and J.-H. Kim. J. Ceram. Process Res. S21 (2020) 9-15.
11. W.H. Kim and S.G. Kang. J. Ceram. Process Res. 11[5] (2010) 557-560.
12. R. Souag, N.-E Kamel, D. Moudir, Y. Mouheb, and F. Aouchiche, J. Ceram. Process Res. 23[3] (2022) 304-311.
13. A. Benedetti, G. Cocco, and G. Fagherazzi, J. Mater Sci. 18 (1983) 1039-1048.
14. M. Sheikhattar, H. Attar, S. Sharafi, and W.M. Carty, Mater. Charact. 118 (2016) 570-574.
15. S.S. Danewalia, S. Kaur, N. Bansal, S. Khan, and K. Singh, J. Non-Cryst. Solids 513 (2019) 64-69.
16. M. Kiani Zitani, S. Banijamali, C. Rüssel, S. Khabbaz Abkenar, P. Mokhtari, H. Ren, and T. Ebadzadeh, J. Asian Ceram. Soc. 8[2] (2020) 234-244.
17. H. Shao, K. Liang, F. Zhou, G. Wang, and A. Hu, 40 (2005) 499-506.
18. G. H. Beall, J. Non-Cryst. Solids 129[1-3] (1991) 163-173.
19. S. Wang, X. Li, C. Wang, M. Bai, X. Zhou, X. Zhang, and Y. Wang, J. Eur. Ceram. Soc. 42[3] (2022) 1132-1140.
20. S. Banijamali, Ceram. Int. 39[8] (2013) 8815-8822.
21. H. Zhan, C. Wu, C. Deng, X. Li, Z. Xie, C. Wang, and Z. Chen, J. Eur. Ceram. Soc. 39 (2019) 1668-1674.
22. R.A. Eppler, J. Am. Ceram. Soc. 52 (1969) 89-94.
23. S. Teixeira and A. Bernardin, Dyes Pigm. 80 (2009) 292-296.
24. E. Bou, A. Moreno, A. Escardino, and A. Gozalbo, J. Eur. Ceram. Soc. 27[2-3] (2007) 1791-1796.
25. S.K. Chen and H.S. Liu, J. Mater. Sci. 29 (1994) 2921-2930.
26. N. Miyata and H. Jinno, J. Mater. Sci. 17[9] (1982) 2693-2699.
27. T. Fuss, A. Moguš-Milanković, C.S. Ray, C.E. Lesher, R. Youngman, and D.E. Day, J. Non-Cryst. Solids 352 (2006) 4101-4111.
28. E.A. De Maeyer, R.M. Verbeeck, and C.W. Vercruysse, J. Dent. Res. 81 (2002) 552-555.
29. M. Zhang, E.K.H. Salje, U. Bismayer, H.G. Unruh, B. Wruck, and C. Schmidt, Phys. Chem. Miner. 22 (1995) 41-49.
30. B.O. Mysen and D. Virgo, Am. Mineral. 65 (1980) 885-899.
31. M. Ma, W. Ni, Y. Wang, Z. Wang, and F.J. Liu, Non-Cryst. Solids 354[52-54] (2008) 5395-5401.
32. L. Deng, F. Yun, R. Jia, H. Li, X. Jia, Y. Shi, and X. Zhang, Mater. Chem. Phys. 239 (2020) 122039.
33. M. Zhao, J. Cao, Z. Wang, and G. Li, J. Non-Cryst. Solids 513 (2019) 144-151.
34. X. Wence, C. Zhao, M. Rui, W. Nannan, and O. Shunli, J. Ceram. Process Res. 24[3] (2023) 512-524.
35. W. Wang, S. Dai, L. Zhou, J. Zhang, W. Tian, and J. Xu, Ceram. Int. 46[3] (2020) 3631-3636.